Chinese Chemical Letters 34 (2023) 107581

Contents lists available at ScienceDirect

Chinese Chemical Letters

journal homepage: www.elsevier.com/locate/cclet

A promising controllable CO_2 capture and separation materials for $CO_2/CH_4/H_2$ under electric field

Chaozheng He [a,*], Houyong Yang [a], Ling Fu [b,*]

[a] Shaanxi Key Laboratory of Optoelectronic Functional Materials and Devices, Institute of Environment and Energy Catalysis, School of Materials Science and Chemical Engineering, Xi'an Technological University, Xi'an 710021, China
[b] College of Resources and Environmental Engineering, Tianshui Normal University, Tianshui 741001, China

ARTICLE INFO

Article history:
Received 11 April 2022
Revised 6 May 2022
Accepted 1 June 2022
Available online 4 June 2022

Keywords:
CO_2 capture
Electric-field controlled
$CO_2/CH_4/H_2$ mixture sequestration
Density functional theory
Two-dimensional materials

ABSTRACT

As the greenhouse effect concerns increases, the development of new materials for the efficient capture and separation of CO_2 gas from gas mixtures has become a matter of urgency. In this study, we performed density functional theory (DFT) calculations to investigate the adsorption and separation behavior of $CO_2/CH_4/H_2$ on the surface of two-dimensional (2D) Al_2C materials under positive/negative applied electric fields. In the absence of an electric field CO_2 is weakly physisorbed on the Al_2C surface, but with the application of an applied electric field, the adsorption state of CO_2 gradually changes from physical to chemisorption (adsorption energy changes from −0.29 eV to −3.61 eV), while the negative electric field has little effect on the adsorption of CO_2. We conclude that the C=O bond in adsorbed CO_2 can be activated under an external electric field (maximum activation of 15% under an external electric field of 0–0.005 a.u.). Only in the presence of an applied electric field of 0.0033 a.u. and temperatures above 525 K/675 K can the adsorption/separation reaction of CO_2 single adsorption and $CO_2/CH_4/H_2$ mixture be spontaneous. The adsorption/desorption of CO_2 on Al_2C nanosheet in an electric field of 0.003–0.0033 a.u. is all exothermic, which can be easily controlled by switching on/off the electric field without any energy barriers. The capacity of Al_2C to capture CO_2 per unit electric field decreases with increasing CO_2 concentration, but still has efficient gas separation properties for $CO_2/CH_4/H_2$. Our theoretical results could provide guidance for designing high-capacity and high-selectivity CO_2 capture materials.

Carbon dioxide (CO_2) capture is now a major concern due to global warming caused by the increasing concentration of CO_2 in the atmosphere, resulting in huge environmental problems due to global climate change [1,2]. Therefore, the most effective and direct way to reduce the concentration of CO_2 in the air is to use adsorbent materials for the direct adsorption and further processing of CO_2 reduction of CO_2 into high value-added products [3–8], which is of great importance for the protection of the environment and has therefore attracted the efforts of many researchers [3,9–11]. Recently, liquid ammonia has been considered an effective way of absorbing CO_2, but this has been limited by the difficulties of CO_2 recovery, its rather low efficiency, its dependence on equipment, and its toxicity [12]. As a result, scientists have put a lot of effort into finding other more environmentally friendly, efficient, energy-saving, and cost-effective methods of capturing and separating CO_2.

At present, the mainstream CO_2 adsorbents are metal-organic frameworks (MOFs) [13,14], covalent organic frameworks (COFs) [15], 2D solid materials such as graphene [16], graphene-like materials such as ZnO [17], Bi cluster [18], porous carbon materials and polymers [16,19,20]. In order to enhance the adsorption capacity and selection sensitivity of adsorbent materials for CO_2, common effective strategies include doping [21–23], chemical functionalisation [14,24–27], and external electric field modulation [28–31], building composites [32–34]. However, a common problem with all these current adsorbents is that the desorption of CO_2 requires relatively high temperatures, which corresponds to high energy consumption [35,36]. It is therefore necessary to develop adsorbents with a high CO_2 capture capacity while at the same time considering the recycling of CO_2 and thus improving the efficiency of the adsorbent [3,4,37].

Recently, Guo *et al.* developed highly efficient sorbent materials for CO_2 separation and capture from the gas mixture under an external electric field on hexagonal boron nitride sheet (h-BN), which can become an effective sorbent for CO_2 capture [38]. Tan *et al.* performed first-principle calculations to propose hybrid h-

* Corresponding authors.
E-mail addresses: hecz2019@xatu.edu.cn (C. He), ful263@nenu.edu.cn (L. Fu).

https://doi.org/10.1016/j.cclet.2022.06.004
1001-8417/

BN-graphene (hybrid BN/G) nanosheets as an experimentally feasible strategy to induce a charge on h-BN for charge-controlled CO_2 capture and high selectivity for separating CO_2 from mixtures with $CH_4/N_2/H_2$ [39]. These demonstrate that the gas separation properties of the material can be effectively improved by the application of an electric field and that it is also possible to recycle the gas by switching off the electric field [29,40–43]. As we all know CO_2 acts as a Lewis acid and is easy to gain an electron rather than donating an electron [3]. Once, if we remove the additional electric field, the adsorbed gas mixtures can be easily desorbed.

Many of the adsorbents that capture CO_2 are two-dimensional materials [44], and the search for new two-dimensional materials with large specific surface areas and high stability is a pressing need in current technological developments (including photocatalytic/thermodynamics catalytic processes [45–51], gas-sensitive core components [52], electrode materials, energy storage, and electronic devices [53], nitrogen reduction reaction [48,52,54–56], hydrogen evolution reaction [57,58], water spiting [59–61]. Recently, researchers were motivated to find a stable planer structure of the Al_2C monolayer, which suggested that the (100) or (010) surface of PdO may be ideal substrates to grow the Al_2C [62]. The planar structure of Al_2C monolayer including two Al and one C atom per unit cell forms the planar tetracoordinate carbon (PTC) structure in which each C atom is surrounded by four Al atoms, which is worth noting that PTC-containing Al_2C monolayer as the global 2D structure, strengthens its great potential for synthesis and identification in experimental realization [62]. Dai *et al.* found that Al_2C monolayers are semiconducting with a bandgap of 1.05 eV (based on HSE06 calculation), a value suitable for photovoltaic applications, and the near-perfect match in lattice constants between the Al_2C monolayer and PdO (100) surface suggests a strong likelihood of experimental realization of the Al_2C monolayer on the PdO (100) substrate [63]. Xu *et al.* reported that the intrinsic acoustic-phonon-limited carrier mobility (μ) of Al_2C monolayer sheet and nanoribbon are investigated using *ab initio* computation and deformation potential theory [64]. Almeida *et al.* investigated hydrogen evolution reaction (HER) and oxygen evolution reaction (OER) [65] on a two-dimensional Al_2C monolayer, revealing the bifunctional catalytic activity of Al_2C [66]. It has also been reported that Al_2C nanosheets have good gas-sensitive properties of toxic volatile organic compounds (VOCs) [67] and hydrogen storage properties after modification with Li atoms [68].

In this study, we specifically provided a detailed description of the adsorption and separation behavior of $CO_2/CH_4/H_2$ on the surface of two-dimensional (2D) Al_2C materials under positive/negative applied electric fields. electric field CO_2 is weakly physisorbed on the Al_2C surface without an electric field, but with the application of an applied electric field, the adsorption state of CO_2 gradually changes from physical to chemisorption (adsorption energy changes from −0.29 eV to −3.61 eV), while the negative electric field has no effect on the adsorption of CO_2. Next, we investigated the behavior of CO_2 adsorption by negative electric fields and the thermodynamic properties of the adsorption process. In addition, the capacity of $A_{l2}C$ to trap CO_2 under an external electric field is also explained in detail.

All the spin-polarized structure optimization calculations are performed using the Dmol^3 procedure [69] based on density generalized theory. The Kohn-Sham equation used in solving the electron density utilizes the generalized gradient approximation (GGA) accompanied by the Perdew-Burke-Ernzerhof (PBE) [70] to describe the exchange-correlation energy functional. To correct for the weaker van der Waals (vdW) [71] interactions between the layered materials Grimme method for DFT-D correction [71] is applied all the time. The double numerical basis set with the D-polarization function (DNP) and the cutoff radius in real space at 4.8 Å. The Al_2C nanosheet was simulated by a 2×3 periodic supercell of size 10.178×9.171 Å, containing 12 Al atoms and 6 C atoms. In addition, a vacuum layer of 15 Å was set in the *z*-axis direction to avoid serious layer-to-layer effects. The convergence criteria of total energy, atomic force, and the maximum displacement were set to 1×10^{-6} Ha, 0.002 Ha/Å and 0.005 Å, respectively. A grid of $3 \times 5 \times 1$ Monkhorst-Pack k-points [72] was employed for the Brillouin zone. The charge analysis is carried out by Hirshfeld charge analysis. The ability to capture CO_2 was studied by variations of thermodynamic functions such as enthalpy (ΔH), entropy (ΔS), and free Gibbs energy (ΔG). Here, we define the adsorption energies (E_{ads}) to describe the interaction between $CO_2/CH_4/H_2$ and the BC_3 sheets as:

$$E_{ads} = E_{g-Al_2C} - E_{Al_2C} - E_g \quad (1)$$

where E_{g-Al_2C}, E_{Al_2C} and E_g represent the total energy of the adsorption of $CO_2/CH_4/H_2$, pristine Al_2C nanosheet, the small molecule during adsorption, respectively. It can be known from the definition that the larger the adsorption energy, the better the adsorption performance. It is worth noting that the positive E-field is perpendiculars to the Al_2C surface and points downward.

Al_2C nanosheets are two-dimensional layered semiconductors with an indirect bandgap of 1.05 eV and two kinds of bond lengths corresponding to 1.965 and 2.570 Å for C-Al and Al-Al bonds in the absence of an applied electric field (Figs. 1a and b) as previously studied in the literature, respectively. In addition, the structure of Al_2C is characterized by two types of rings, C_2Al_2 tetrads, and C_2Al_4 hexads. The stability of the structure under electric field needs to be verified before the gas adsorption test, so the Al_2C structure was selected in the electric field range from −0.005 a.u. to 0.005 a.u. The stability of Al_2C under electric field is discussed in terms of energy, kinetic and thermodynamic stability. The energy stability is illustrated by the following equation for the cohesive energy:

$$E_{coh} = \frac{mE_{Al} - nE_C - E_{Al_2C}}{m + n} \quad (2)$$

where E_{Al} and E_C refer to the energy of individual Al and C atoms, E_{Al_2C} refers to the energy of Al_2C in the supercell, and *m* and *n* refer to the number of Al and C atoms, respectively. As shown in Fig. 1b, there is regularity in the stability of Al_2C under the electric field from −0.005 a.u. to 0.005 a.u. When the electric field value increases from 0 a.u. to 0.005 a.u., the cohesive energy of Al_2C increases from 4.3414 eV to 4.3447 eV with an increase of 0.033 eV, which indicates that the positive electric field can increase the structural stability of Al_2C. Similarly, it can be seen from Fig. 1b that the negative electric field can also increase the structural stability of Al_2C. The Al_2C structure has the same cohesive energy for the same intensity of positive and negative electric field values. These values of aggregation energy can be compared to graphene (6.93–7.21 eV) and penta-graphene (6.86–7.21 eV), demonstrating the high stability of Al_2C. Furthermore, Al_2C nanosheet with an electric field of 0.005 a.u. is performed a canonical ensemble at 300 K for *ab initio* molecular dynamics (AIMD) simulation. After 2 ps with a time step of 1 fs (Figs. 1c and f), the Al_2C systems retain their stable structures under 0.005 a.u. electric field, as shown in Fig. 1e. These findings demonstrate the stability of the Al_2C nanosheet in an applied electric field. Next, we tested the adsorption of CO_2 at different electric field values. Before the test, we selected six adsorption sites depending on the chemical environment of the atoms, as shown in Fig. 1a.

As shown in Fig. S1 (Supporting information), in the absence of an applied electric field, neither $CO_2/CH_4/H_2$ can be chemically adsorbed on the surface of Al_2C. The adsorption energies of CO_2 and CH_4 are −0.29 eV and −0.24 eV, respectively, which are relatively weak physical adsorption, but the adsorption energy of H_2 is −0.11 eV indicating that H_2 cannot be adsorbed on the

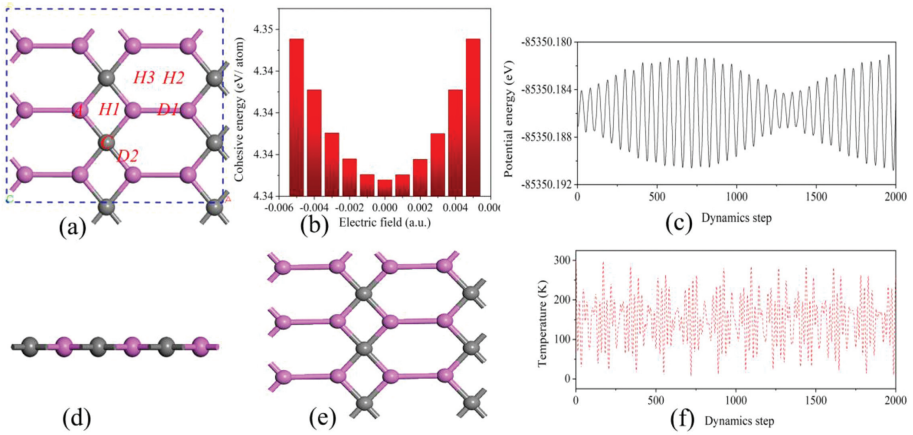

Fig. 1. (a) Top (upper) and (d) side (lower) views of Al_2C structure (2×3). C, H1, H2, H3, D1, D2 denote different adsorption sites on Al_2C. Al atoms and C atoms are in magenta and gray, respectively. (b) The cohesive energy of Al_2C nanosheet in an applied electric field. (c) Energy change and (f) temperature during molecular dynamics simulation of Al_2C after 2000 fs at 300 K with an external electric field of 0.005 a.u. and (e) structure after 2000 ps at 300 K simulation.

Al_2C surface. The most stable adsorption structures of H_2 and CH_4 (Figs. S1b and c) show that the distance of the small molecules from the surface is 2.863 and 3.148 Å, respectively. It is that all three gas molecules are readily present on the H ring vacancies site. Table S1 (Supporting information) presents the corresponding adsorption energy E_{ads} (eV), minimum distance D_m (Å) between the gas molecule and Al_2C substrate, bond length (Å) and angle after gas adsorption, total Hirshfeld-type charge (e^-)of the gas molecule (ΔQ) without an electric field. All the bond lengths are in angstroms. All the data in the Table S2 (Supporting information) prove that in the absence of an applied electric field, $CO_2/CH_4/H_2$ is not chemisorbed on the Al_2C surface, and the interaction between the gas molecules and the Al_2C surface is too weak to achieve the separation of the gases according to the adsorption difference.

To explore whether the adsorption of CO_2 on the Al_2C surface can be regulated by the applied electric field, we investigated all possible adsorption structures of CO_2 on the Al_2C surface under positive and negative gradient electric fields (Fig. S2 in Supporting information). Comparing the adsorption configuration of CO_2 in Fig. S2 when no/0.001 a.u. electric field is applied, it can be found that the bond angle of CO_2 is slightly changed from 178.6° to 178.3° and the corresponding shortest adsorption distance is reduced from 3.156 Å to 3.123 Å. The Hirshfeld-charge transferred from Al_2C to CO_2 is reduced from 0.021 e^- to 0.007 e^-. The corresponding adsorption energy increases from −0.29 eV to −0.31 eV, indicating that the electric field at this point enhances the interaction between CO_2 and A_2C but it is still physical adsorption.

Table S3 (Supporting information) presents the structural parameters, including the O–C-O angles, C–O bond length, the electron transfers from Al_2C nanosheet to CO_2, C–O bond length change rate, the distance between CO_2 and surface in an applied electric field. When the electric field value increases to 0.003 a.u., the molecular conformation of CO_2 still does not change significantly (Fig. S2c). The C–O bond length at this point is 1.176 Å, the bond angle is 175.6°, and the corresponding adsorption energy is −0.47 eV. However, when the electric field value increases to 0.0033 a.u., the bond angle of CO_2 is sharply bent to 121.5°, the C–O bond length is stretched to 1.314 Å, and the shortest adsorption distance of CO_2 from the A_2C surface is shortened to 1.416 Å, with Hirshfeld-charge −0.496 e^-, corresponding to adsorption energy of −3.06 eV. These evidences lead to CO_2 on the Al_2C surface to a relatively strong chemisorption. As shown in Figs. S2a–c, the critical point of CO_2 from physical adsorption to chemical adsorption on the Al_2C substrate is between 0.003–0.0033 a.u. Previous studies in the literature have shown that the minimum E-field value (0.0065 a.u.) required for the conversion of CO_2 from physical adsorption to chemical adsorption is much smaller than that of Penta-graphene (0.025–0.03 a.u.) [30], and is also smaller than the E-field value required in the previous literature to capture CO_2 materials, such as C_2N (0.035–0.04 a.u.), h-BN (0.01–0.03 a.u.) [38], C_3N (0.032–0.037 a.u.) [73], P-doped C_{60} (0.008 a.u.) [29], P-doped graphene (0.013 a.u.) [74], and BC_3 (0.006–0.0065 a.u.) [11]. However, the critical E-field value of this CO_2 from physical adsorption to chemical adsorption is greater than that of MoS_2 (0.004 a.u.) [75] and PC_5 (0.002 a.u.) [31] because the polarization effect of the Al_2C structure under the E-field is not as strong as the former two, which shows that Al_2C captures CO_2 in this way is more economical and efficient. Figs. S2e and f illustrate that when the applied electric field is further increased to 0.005 a.u., the bond angle bending of CO_2 further increases from 121.5° to 120.3°, the adsorption distance decreases from 1.461 Å to 1.181 Å, and the C–O bond length stretches from 1.314 Å to 1.325 Å. It is worth noting that the charge of CO_2 is −0.597 e^- and the corresponding adsorption energy increases to −6.50 eV. The above evidence indicates that with the increase of the positive electric field strength, the interaction between CO_2 and Al_2C surface is enhanced and the chemisorption intensity of CO_2 becomes higher and higher.

We also investigated the effect of the negative (upward perpendicular to the *z*-axis) electric field on the adsorption of CO_2 on the Al_2C surface. As shown in Figs. S2g–k, when the electric field value increases from −0.001 a.u. to −0.005 a.u., it is obvious that all the molecular conformational change of CO_2 is negligible, but there is a slight increase in the bond angle of CO_2 (to 179.3° which is close to the bond angle of gaseous CO_2 molecules). This indicates that the effect of negative electric field and positive electric field on the nature of CO_2 adsorption by Al_2C is different, and the negative electric field cannot change the nature of CO_2 adsorption. But why the positive electric field can significantly promote the adsorption of CO_2 on the surface of Al_2C. We will then look for the reason through a more in-depth electronic structure analysis.

In order to gain insight into the reasons for the enhanced binding energy of CO_2 to Al_2C under electric field, the charge density difference and density of states (DOS) analyzes are performed. Fig. S3 (Supporting information) shows the charge difference density of the most stable structure of CO_2 adsorbed on the Al_2C surface in the external electric field range −0.005 a.u. to 0.005 a.u. Figs. S3a–c show that between the electric field of 0.001–0.003 a.u. CO_2 prefers to get electrons from the substrate and that there is a flow of electrons within the CO_2 molecule under the applied electric field (the flow direction is from C atoms to O atoms), which is consistent with the Hirshfeld-charge analysis in Table S3. The

blue region between the CO_2 molecule and the substrate indicates an increase in the electron density in this region which leads to enhanced interaction between the two. However, as the electric field strength increases to 0.0033–0.005 a.u., the electron density near the CO_2 molecule increases as seen in Figs. S3d–f, indicating that more electrons are transferred from the substrate to the CO_2 molecule as the electric field strength increases. CO_2 is a Lewis acid molecule and tends to accept electrons. The results of the charge density indicate that the positive electric field favors the contribution of electrons from Al_2C to CO_2, thus activating CO_2. At the same time, the interaction between CO_2 and Al_2C is enhanced because more electrons are coupled between the O-Al bonds thus forming stronger bonds, explaining why the adsorption of CO_2 on the Al_2C surface is enhanced with increasing electric field strength. When the electric field is between −0.005 a.u. and 0 a.u., as depicted in Figs. S3g–l, there is no remarkable change in the distribution of electron density, so we conclude that the negative electric field does not significantly affect the electron distribution of the system.

In order to study the alteration of C=O bond interactions in CO_2 molecules under electric fields, we further investigated the Crystal Orbital Hamiltonian Population (COHP) [76] of C=O bonds to analyze the interaction between C=O. Fig. S3 depicted the partial density of states (PDOS) and molecular orbital of CO_2 molecule adsorbed on Al_2C under different electric field values, above and below the 0 value of COHP are the anti-bonding state and bonding state, respectively. Yellow stands for bonding contributions, while cyan stands for antibonding contributions. In Figs. S3a and b by comparing the PDOS and COHP of C=O bonds under 0 a.u. and 0.003 a.u. electric fields, it can be found that the bonding molecular orbitals of C=O without electric field are mainly localized at the energy level of −8.3 eV and consist mainly of O p, O s, and C p orbitals contributing to each other. The C=O and antibonding molecular orbitals (the contribution of C p orbitals dominant) in the absence of electric field are mainly composed of C p orbitals and O p orbitals. The molecular orbitals of the C=O bond at 0.003 a.u. show hardly ever switch, because the electric field strength is not large enough to reach the critical value for the rearrangement of the C=O bond molecular orbitals. However, when the electric field value increases to 0.0033 a.u., a noteworthy change in the molecular orbitals, as well as the composition of C=O can be seen.

As shown in Figs. S4c and d (Supporting information), firstly, the molecular orbitals of the C=O bond below the Fermi energy level and the corresponding PDOS have a significant shift to a shallower energy level, and the bonding molecular orbitals of C=O have a cleavage leading to a significant decrease in the bonding strength. It is noteworthy that the antibonding orbital of the C=O bond moves to deeper energy levels (from 3.2 eV to 2.5 eV) and the area of the antibonding state increases, indicating that more empty orbitals constitute the antibonding orbital. It is interesting to note that the atomic orbitals constituting the bonding orbitals of the C=O bond at 0.004 a.u. electric field form two more prominent peaks at −1.8 eV and −2.3 eV, which are below the Fermi energy level but do not contribute to the bonding. Integrated COHP (ICOHP) was calculated by calculating the energy integral up to the highest occupied bands, and the value of ICOHP quantitatively reflected the strength of bonding. As shown in Fig. S4 (Supporting information), the value of ICOHP decreases with increasing electric field strength, which indicates that the bonding strength of the C=O bond decreases and the applied electric field can significantly activate the C=O bond but there is a minimum electric field strength of 0.0033 a.u. The above evidence also indicates that the applied positive electric field can effectively activate the C=O bond in CO_2.

In order to gain a deeper understanding of the mechanism of CO_2 adsorption on the Al_2C surface, we investigated the mechanism of CO_2 adsorption on the Al_2C surface under different electric field strengths. In the absence of electric field, as shown in Fig. S5a (Supporting information), the 2s and 2p orbitals of CO_2 molecules near the Fermi energy level have almost no overlap with the 2p orbitals of Al atoms and the 2p orbitals of C. This indicates that the interaction between the three is so weak that CO_2 molecules cannot be chemisorbed on the Al_2C surface. Fig. S5b (Supporting information) shows the PDOS under 0.002 a.u. electric field, which is similar to the case without applied electric field when the overlap of the three electronic density of states is very small. However, when the electric field value increases to 0.003 a.u., the overlap between C 2p and CO_2 2s begins to appear in the −5∼0 eV energy range, which indicates that the interaction between C atoms and CO_2 begins to increase at this time in response to the electric field. The above results indicate that the applied electric field significantly promotes the interaction of CO_2 with Al and C atoms on the surface of Al_2C, and Al and C atoms synergistically exhibit chemisorption effect on CO_2 under electric field.

To evaluate the effect of CO_2 adsorption on the Al_2C surface and to visualize the effect of the applied electric field on CO_2 adsorption, we used the structural parameters, including (a) the O–C-O angles, (b) C–O bond length, (c) the electron transfers from Al_2C nanosheet to CO_2, (d) C–O bond length change rate, (e) distance between CO_2 and surface, and (f) the adsorption energy of the most stable configurations in an applied electric field as a function of the electric field value, as depicted in Fig. S6 (Supporting information). Both C–O bond length change rate and C–O bond length increase considerably with increasing electric field strength while there is a tendency that the O–C-O angles, the electron transfers from Al_2C nanosheet to CO_2, the distance between CO_2 and surface, and the adsorption energy of CO_2 decrease due to an increasing electric field strength, which can be interpreted by the increasing static electric field generated near the surface of the charged sorbent because of increasing electric field. Moreover, the increasing electron transfers from Al_2C nanosheet to CO_2 and the decreasing distance between CO_2 molecule and the surface contribute to the enhanced adsorption energy of CO_2 molecule (Figs. S6c and e). Therefore, we can conclude that polarization of CO_2 molecule induced by electric field has an impact on adsorption energy of CO_2 molecule, demonstrating its significant role in electric field-controlled switchable CO_2 capture.

To study the thermodynamic properties of CO_2 adsorption on the Al_2C with an applied electric field 0/0.0033 a.u., the formation of chemisorbed configurations at different temperatures, changes in the entropy of thermodynamic functions (ΔS, cal mol^{-1} K^{-1}), enthalpy (ΔH, kcal/mol), and Gibbs free energy (ΔG, kcal/mol) with temperature (K) were explored. Fig. S7 (Supporting information) illustrates the thermodynamic properties of CO_2 single adsorption and $CO_2/CH_4/H_2$ mixed gas adsorption with an applied electric field of 0.0033 a.u. on the Al_2C as a function of temperatures (K). For CO_2 adsorption alone under an electric field of 0.0033 a.u., the thermodynamic properties are shown in Fig. S7a. Capacity volume (Cv) increases with temperature in the temperature range of 0–525 K but slowly converges to a constant between 525 K and 1000 K. ΔS and ΔH increase with temperature in the range of 0–1000 K. The temperature of Cv increases with temperature in the range of 0–1000 K. The temperature of Cv increases with temperature in the range of 0–1000 K. It is noteworthy that ΔG in the chemical process of adsorption of individual CO_2 molecules under an electric field of 0.0033 a.u. is greater than zero in the temperature range of 0–525 K, but less than zero in the temperature range of 525–1000 K. This suggests that the chemisorption of individual CO_2 on the Al_2C surface is only spontaneous at temperatures greater than 525 K. Fig. S7b depicted the thermodynamic properties of $CO_2/CH_4/H_2$ mixtures adsorption under an electric field of 0.0033 a.u. The trends of *S*, *H*, and Cv in the

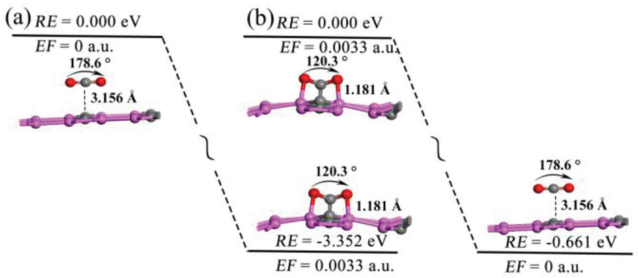

Fig. 2. The energy profile for the chemisorption to physisorption of the adsorbed CO_2 over Al_2C due to removing or switching of electric field (EF = 0.0033 a.u.).

thermodynamic parameters of $CH_2/CH_4/H_2$ mixed gas adsorption under 0.0033 a.u. applied electric fields are consistent with those of the CO_2 adsorption system alone, with the difference that the ΔG of the mixed gas system adsorption is only greater than 0 between 0 and 675 K. This indicates that only at temperatures greater than 675 K, the mixed gas adsorption under 0.0033 a.u. electric field the behavior of separation can be spontaneous.

In order to explore the reaction mechanism of the CO_2 adsorption reaction on Al_2C under the influence of an applying external electric field, we have studied the reaction of CO_2 capture/release on the Al_2C nanosheet by turning on/off an external electric field 0.0033 a.u. As shown in Fig. 2a, the CO_2 molecule is chemisorbed on the Al_2C with a C–O distance of 1.181 Å under influence of an applied 0.0033 a.u. electric field. The process has no activation barrier and the reaction is exothermic by −3.352 eV. The conversion process of the chemisorption to physisorption was studied when the external electric field is switched off. The results show that the conversion process (desorption process) is exothermic by −0.661 eV without an activation barrier (Fig. 2b). These studies show that we can control the capture/release of CO_2 /from Al_2C nanosheet by simply switching on/off the external electric field.

The CO_2 capture capacity is an important criterion of the performance of an adsorbent, so we scrutinize the number of CO_2 molecules that could be captured by the Al_2C laminate for electric field strengths ranging from 0 to 0.005 a.u., as depicted in Fig. 3. It is clear that when the coverage of CO_2 molecules is relatively low (Figs. 3a–c), CO_2 can be chemisorbed on the Al_2C surface at an electric field of 0.003–0.004 a.u. It is noteworthy that when 2 CO_2 molecules are adsorbed on the substrate, the CO_2 capture rate at an electric field of 0.003 a.u. is 50%. As the CO_2 coverage increases, we find that the capacity of Al_2C to capture CO_2 is limited, corresponding to a definite value for the amount of CO_2 captured. For the adsorption of 4 CO_2 molecules, the percentage of CO_2 captured is 25% when the electric field value is between 0.003 a.u. and 0.004 a.u., and when the electric field continues to increase to 0.005 a.u. the capacity to capture CO_2 at this point is 50%. When the CO_2 coverage is 5, the CO_2 capture capacity between 0.003 a.u. and 0.004 a.u. is 20% and the maximum capture capacity in the tested range is 3 CO_2 molecules (75%). When the CO_2 coverage is further increased until 100% of the adsorption active sites are utilized, we find that the CO_2 capture capacity is then 0. In this section, we investigate the capacity of Al_2C to trap CO_2 under an electric field by studying the increase in CO_2 concentration in the atmosphere by increasing the amount of CO_2 in a specific electric field range, based on the number of CO_2 molecules that can be chemisorbed. In summary, the ability of Al_2C to capture CO_2 under an electric field decreases with increasing CO_2 concentration, which is quite understandable since the average energy gained per CO_2 per unit electric field decreases with increasing CO_2 concentration.

Not only is the capture capacity important for CO_2 adsorbents, but also the separation of the gas according to the selectivity of the adsorbent is equally important. In industrial natural gas processing, there is a gas mixture $CO_2/CH_4/H_2$, where CH_4 and H_2 are clean energy sources and CO_2 as an impurity can affect the purity of the energy gas. We have therefore investigated the application of Al_2C for gas separation and purification based on the selective difference in the adsorption of $CO_2/CH_4/H_2$ by Al_2C under an applied electric field. The optimized most stable structure of $CO_2/CH_4/H_2$ under an applied electric field of 0.0033 a.u. is shown in Fig. S8 (Supporting information), corresponding to adsorption energies of −3.61, −0.41 and −0.37 eV, respectively. The difference in the adsorption behavior of the gas mixture is also evidenced by the difference in charge density shown in Fig. S9 (Supporting information). The adsorption behavior of $CO_2/CH_4/H_2$ gas on the Al_2C surface in the electric field range of 0–0.005 a.u. was also investigated and the adsorption energy of the gas mixture was fitted with the applied electric field strength as the horizontal coordinate, as shown in Fig. 4. Fig. 4a shows that the adsorption energy of $CO_2/H_2/CH_4$ below −0.5 eV at 0–0.003 a.u. The three components of the gas mixture are physically adsorbed, which can not achieve effective gas separation. However, as the electric field strength increases, we find that the corresponding CO_2 adsorption is most intense showing an exponential increase, but between 0.003 a.u. and 0.0035 a.u. CH_4/H_2 is still physically adsorbed. This

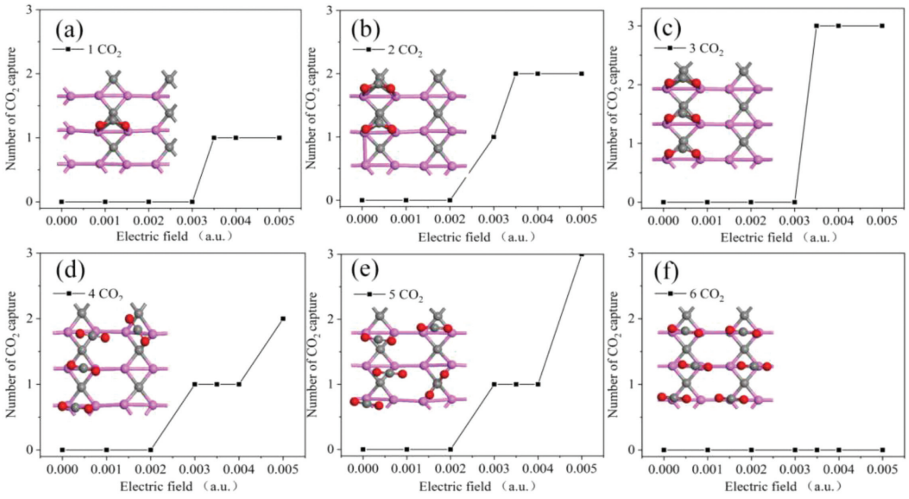

Fig. 3. (a–f) The number of CO_2 molecules captured with different positive electric field from 0 to 0.005 a.u. and corresponding structure.

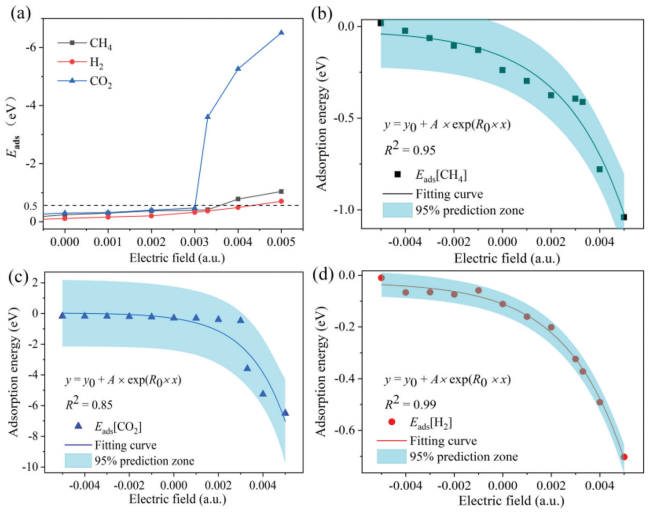

Fig. 4. (a) The adsorption energies of the most stable configurations of CO_2, H_2, and CH_4 on Al_2C nanosheet in an applied electric field. The fitted tendency between electric field values and adsorption energies of (b) CH_4, (c) CO_2 and (d) H_2. The fitted functions are written in the figures.

significant difference in adsorption allows for efficient $CO_2/CH_4/H$ gas separation. In contrast, the correlation between the adsorption energy of CO_2 and the electric field is weaker, and the correlation between the adsorption energy of CH_4 and the electric field is even weaker (Figs. 4b–d).

The separation and mix purification of Al_2C nanosheet materials using the difference of adsorption properties of $CO_2/CH_4/H_2$ gas mixtures under an applied electric field has been calculated theoretically using the first principles. The main points are summarized as follows:

(1) In the absence of an electric field CO_2 is weakly physisorbed on the Al_2C surface, but with the application of an applied electric field, the adsorption state of CO_2 gradually changes from physical to chemisorption (adsorption energy changes from −0.29 eV to −3.61 eV) with increasing electric field strength, with the required electric field critical range of 0.003–0.0033 a.u. However, a negative electric field has little effect on the adsorption of CO_2.

(2) The C=O bond in adsorbed CO_2 has a significant activation effect under an external electric field (maximum activation of 15% under an external electric field of 0–0.005 a.u.) because the applied electric field enhances the polarization of the CO_2 molecules and changes the molecular orbital electron distribution of CO_2.

(3) Only in the presence of an applied electric field of 0.0033 a.u. and temperatures above 525/675 K can the adsorption/separation reaction of (a) CO_2 single adsorption and (b) $CO_2/CH_4/H_2$ mixture to be spontaneous. The adsorption/desorption of CO_2 on Al_2C nanosheet in an electric field of 0.003–0.0033 a.u. are all exothermic, which can be easily controlled by switching on/off the electric field without any energy barriers.

(4) The capacity of Al_2C to capture CO_2 per unit electric field decreases with increasing CO_2 concentration but still has efficient gas separation properties for $CO_2/CH_4/H_2$.

Declaration of competing interest

The authors declare that they have no known competing financial interests or personal relationships that could have appeared to influence the work reported in this paper.

Acknowledgments

This study was funded by the National Natural Science Foundation of China (No. 21603109), the Henan Joint Fund of the National Natural Science Foundation of China (No. U1404216), and the Scientific Research Program Funded by Shaanxi Provincial Education Department (No. 20JK0676).

Supplementary materials

Supplementary material associated with this article can be found, in the online version, at doi:10.1016/j.cclet.2022.06.004.

References

[1] E.S. Sanz-Pérez, C.R. Murdock, S.A. Didas, C.W. Jones, Chem. Rev. 116 (2016) 11840–11876.
[2] Q. Li, Y.C. Wang, J. Zeng, et al., Rare Met. 40 (2021) 3442–3453.
[3] Y. Wang, Y. Liu, W. Liu, et al., Energy Environ. Sci. 13 (2020) 4609–4624.
[4] L. Fu, R. Wang, C.X. Zhao, et al., Chem. Eng. J. 414 (2021) 128857.
[5] B. Yang, L. Li, Z. Jia, et al., Chin. Chem. Lett. 31 (2020) 2627–2633.
[6] S. Gong, G. Zhu, R. Wang, et al., Appl. Catal. B: Environ. 297 (2021) 120413.
[7] C.H. Yang, F. Nosheen, Z.C. Zhang, Rare Met. 40 (2021) 1412–1430.
[8] R. Cheng, C.C. Chung, S. Wang, et al., Mater. Today Phys. 17 (2021) 100358.
[9] Q.G. Jiang, Z.M. Ao, S. Li, et al., RSC Adv. 4 (2014) 20290–20296.
[10] C. He, R. Wang, D. Xiang, et al., Appl. Surf. Sci. 509 (2020) 145392.
[11] H. Yang, C. He, L. Fu, et al., Chin. Chem. Lett. 32 (2021) 3202–3206.
[12] Y.S. Bae, R.Q. Snurr, Angew. Chem. Int. Ed. 50 (2011) 11586–11596.
[13] R.A. Agarwal, A.K. Gupta, D. De, Cryst. Growth Des. 19 (2019) 2010–2018.
[14] M. Kang, D.W. Kang, C.S. Hong, Dalton Trans. 48 (2019) 2263–2270.
[15] Y. Zeng, R. Zou, Y. Zhao, Adv. Mater. 28 (2016) 2855–2873.
[16] R.M. del Castillo, A.G. Calles, R. Espejel-Morales, et al., Comput. Condens. Matter 16 (2018) e00315.
[17] G.S. Rao, T. Hussain, M.S. Islam, et al., Nanotechnology 27 (2016) 015502.
[18] Y. Wang, L. Xu, L. Zhan, et al., Nano Energy 92 (2022) 106780.
[19] K.V. Kumar, K. Preuss, L. Lu, et al., J. Phys. Chem. C 119 (2015) 22310–22321.
[20] A. Liu, J. Long, S. Yuan, et al., Phys. Chem. Chem. Phys. 21 (2019) 5133–5141.
[21] E.N.C. Paura, W.F. da Cunha, J.B.L. Martins, et al., RSC Adv. 4 (2014) 28249–28258.
[22] N. Iqbal, X. Wang, A.A. Babar, et al., J. Colloid Interfaces Sci. 476 (2016) 87–93.
[23] Z.X. Wei, Y.T. Zhu, J.Y. Liu, et al., Rare Met. 40 (2021) 767–789.
[24] M. Wang, S. Wei, Z. Wu, et al., Mater. Lett. 230 (2018) 28–31.
[25] A. Bafekry, C. Stampfl, M. Ghergherehchi, Nanotechnology 31 (2020) 295202.
[26] S. Zhou, M. Wang, S. Wei, et al., Mater. Today Phys. 16 (2021) 100301.
[27] S. Zhou, M. Wang, S. Wei, et al., Mater. Today Phys. 21 (2021) 100539.
[28] R. Burgos, J.H. Warnes, J. Magn. Magn. Mater. 498 (2020) 166156.
[29] A.A. Khan, I. Ahmad, R. Ahmad, Chem. Phys. Lett. 742 (2020) 137155.
[30] M. Wang, Z. Zhang, Y. Gong, et al., Appl. Surf. Sci. 502 (2020) 144067.
[31] S. Zhou, M. Wang, J. Wang, et al., J. Mater. Chem. A 8 (2020) 9970–9980.
[32] H. An, B. Feng, S. Su, Carbon 47 (2009) 2396–2405.
[33] S.K. Ryi, J.S. Park, K.R. Hwang, et al., Int. J. Hydrog. Energy 36 (2011) 13769–13775.
[34] S.S. Kazi, A. Aranda, L. di Felice, et al., Energy Proced. 114 (2017) 211–219.
[35] A. Hanif, S. Dasgupta, S. Divekar, et al., Chem. Eng. J. 236 (2014) 91–99.
[36] M. Gunnarsson, D. Bernin, Å. Östlund, et al., Green Chem. 20 (2018) 3279–3286.
[37] C.Z. He, H.T. Wang, L. Fu, et al., Chin. Chem. Lett. 33 (2021) 990–994.
[38] H. Guo, W. Zhang, N. Lu, et al., J. Phys. Chem. C 119 (2015) 6912–6917.
[39] X. Tan, L. Kou, S.C. Smith, ChemSusChem 8 (2015) 2987–2993.
[40] W. Liu, Y.H. Zhao, J. Nguyen, et al., Carbon 47 (2009) 3452–3460.
[41] Z.M. Ao, F.M. Peeters, Appl. Phys. Lett. 96 (2010) 253106.
[42] A.V. Kityk, R. Czaplicki, A. Klopperpieper, et al., Appl. Phys. Lett. 96 (2010) 061911.
[43] Q. Sun, G.Q. Qin, Y.Y. Ma, et al., Nanoscale 9 (2017) 19–24.
[44] Y. Jia, F. Li, K. Fan, et al., Adv. Powder Mater. 1 (2021) 100012.
[45] S.L. Li, X. Kan, L.Y. Gan, et al., Appl. Surf. Sci. 556 (2021) 149779.
[46] Y. Sun, Y. Wang, H. Li, et al., J. Energy Chem. 62 (2021) 51–70.
[47] H. Li, Z. Zhao, Q. Cai, et al., J. Mater. Chem. A 8 (2020) 4533–4543.
[48] H. Yin, L.Y. Gan, P. Wang, J. Mater. Chem. A 8 (2020) 3910–3917.
[49] C. Cao, D.D. Ma, J.F. Gu, et al., Angew. Chem. Int. Ed. 59 (2020) 15014–15020.
[50] J. Han, S. Zhang, Q. Song, et al., Sustain. Energy Fuels 5 (2021) 509–517.
[51] X. Li, J. Liu, J. Huang, et al., Acta Phys. Chim. Sin. 37 (2020) 2010030.
[52] D. Jiao, Y. Liu, Q. Cai, et al., J. Mater. Chem. A 9 (2021) 1240–1251.
[53] W.W. Fu, M. Zhang, Z.R. Shen, Chin. J. Struct. Chem. 40 (2021) 797–805.
[54] C. Liu, Q. Li, C. Wu, et al., J. Am. Chem. Soc. 141 (2019) 2884–2888.
[55] X. Chen, W.J. Ong, X. Zhao, et al., J. Energy Chem. 58 (2021) 577–585.
[56] C. He, J. Wang, L. Fu, et al., Chin. Chem. Lett. 33 (2022) 1051–1057.
[57] L. Xie, L. Wang, W. Zhao, et al., Nat. Chem. 12 (2021) 5070.
[58] Y. Liu, Q. Feng, W. Liu, et al., Nano Energy 81 (2021) 105641.
[59] H. Zhang, W. Wei, S. Wang, et al., J. Mater. Chem. A 9 (2021) 4082–4090.
[60] X.H. Chen, Q. Zhang, L.L. Wu, et al., Mater. Today Phys. 15 (2020) 100268.
[61] H. Jing, P. Zhu, X. Zheng, et al., Adv. Powder Mater. 1 (2021) 100013.

[62] Y. Li, Y. Liao, P.V.R. Schleyer, et al., Nanoscale 6 (2014) 10784–10791.
[63] J. Dai, X. Wu, J. Yang, et al., J. Phys. Chem. Lett. 5 (2014) 2058–2065.
[64] Y. Xu, J. Dai, X.C. Zeng, J. Phys. Chem. Lett. 7 (2016) 302–307.
[65] R.Z. Qin, Y. Wang, Q.H. Zhao, et al., Chin. J. Struct. Chem. 39 (2020) 605–614.
[66] R. Almeida, A. Banerjee, S. Chakraborty, et al., ChemPhysChem 19 (2018) 148–152.
[67] W. Li, Q. Jiang, D. Li, et al., Chin. Chem. Lett. 32 (2021) 2803–2806.
[68] R. Rahimi, M. Solimannejad, Int. J. Quantum Chem. 121 (2021) e26528.
[69] B. Delley, J. Chem. Phys. 113 (2000) 7756–7764.
[70] J.P. Perdew, K. Burke, M. Ernzerhof, Phys. Rev. Lett. 77 (1996) 3865–3868.
[71] S. Grimme, J. Antony, S. Ehrlich, et al., J. Chem. Phys. 132 (2010) 154104.
[72] D.J. Chadi, Phys. Rev. B 16 (1977) 1746–1747.
[73] X. Li, T. Guo, L. Zhu, et al., Chem. Eng. J. 338 (2018) 92–98.
[74] M.D. Esrafili, J. Mol. Graph. Model. 90 (2019) 192–198.
[75] Q. Yue, Z. Shao, S. Chang, et al., Nanoscale Res. Lett. 8 (2013) 425.
[76] V.L. Deringer, A.L. Tchougreeff, R. Dronskowski, J. Phys. Chem. A 115 (2011) 5461–5466.